Energy 246 (2022) 123428

Contents lists available at ScienceDirect

Energy

journal homepage: www.elsevier.com/locate/energy

Optimal energy management for multi-energy multi-microgrid networks considering carbon emission limitations

Xiaoqing Zhong [a, b], Weifeng Zhong [a, c], Yi Liu [a, d], Chao Yang [a, e], Shengli Xie [a, e, *]

[a] School of Automation, Guangdong University of Technology, Guangzhou, 510006, China
[b] Key Laboratory of Intelligent Information Processing and System Integration of IoT, Ministry of Education, Guangzhou, 510006, China
[c] 111 Center for Intelligent Batch Manufacturing Based on IoT Technology, Guangzhou, 510006, China
[d] Guangdong Key Laboratory of IoT Information Technology, Guangzhou, 510006, China
[e] Guangdong-HongKong-Macao Joint Laboratory for Smart Discrete Manufacturing, Guangzhou, 510006, China

ARTICLE INFO

Article history:
Received 10 September 2021
Received in revised form
29 December 2021
Accepted 6 February 2022
Available online 8 February 2022

Keywords:
Multi-energy multi-microgrid network
Distributed electricity sharing
Energy management strategy
Carbon emissions

ABSTRACT

Multi-energy multi-microgrid (MMG) networks are considered as a promising form of energy systems that can integrate various energy resources and improve energy utilization efficiency. Carbon emission limitation, regarded as a significant factor in energy management, has received increasing attention in recent years. By taking into account both economic and environmental factors, MMG networks can offer a great opportunity to reduce operation costs and carbon emissions. In this paper, we propose an optimal energy management strategy for minimizing the operation cost of an MMG network, considering operation constraints and carbon emissions. The energy management strategy is designed to consist of a day-ahead phase and an intra-day phase to overcome the uncertainty effects of renewable energy sources (RESs) generation and load demands. We first present a day-ahead scheduling strategy for the MMG network, in which microgrids operate in a distributed manner and share electricity while preserving their privacy. We then present an intra-day scheduling strategy for each microgrid, in which the operation costs and penalty costs caused by the adjustment of energy devices and energy procurement are minimized sequentially using a rolling horizon method. Simulation results demonstrate the effectiveness of the proposed energy management strategy in lowering operation costs and carbon emissions.

1. Introduction

With the impact of climate change and increasing environmental awareness, the energy sector has been motivated to mitigate carbon emissions and impose carbon emission limitations [1,2]. Under these circumstances, the concept of networked microgrids has been proposed as a promising form of energy systems. In contrast to the conventional concept of microgrids that mainly focuses on the operation of an independent microgrid and its interaction with the utility, networked microgrids are characterized by local energy trading and sharing of renewable energy sources (RESs). Thus, networked microgrids have superiority in enhancing system flexibility, lowering operation costs, and reducing carbon emissions [3–5]. Nowadays, local electricity sharing between microgrids is feasible and is an important energy management method that allows microgrids to sell and buy locally [6]. Many practical systems (e.g., Brooklyn microgrid) that consider the electricity sharing between different microgrids (entities) have been introduced [7]. The energy management of networked microgrids has received a lot of attention in the literature. For example, a Nash bargaining approach is presented in Refs. [4,8] for incentivizing energy trading among microgrids. A peer-to-peer energy sharing model among buildings is proposed in Ref. [5], which minimizes the total energy costs with distributed electricity transactions. Note that the studies in Refs. [4,5,8] only focus on the electricity loads of microgrids, without considering the demands for multiple types of energy (e.g., electricity, natural gas, and heating).

Many existing works have studied economic scheduling problems of multi-energy multi-microgrid (MMG) networks. In Ref. [9], energy sharing among energy hubs is studied under three organized schemes, i.e., individual, sharing market, and aggregation. A

* Corresponding author. School of Automation, Guangdong University of Technology, Guangzhou, 510006, China.
E-mail addresses: xiaoqing_zhong@qq.com (X. Zhong), wfzhongs@gdut.edu.cn (W. Zhong), yi.liu@gdut.edu.cn (Y. Liu), yangchaoscut@aliyun.com (C. Yang), shlxie@gdut.edu.cn (S. Xie).

https://doi.org/10.1016/j.energy.2022.123428
0360-5442/

Nomenclature

Abbreviations

RES	renewable energy source
MMG	multi-energy multi-microgrid
CHP	combined heat and power
GB	gas boiler
HP	heat pump
ES/HS	electric/heat storage
WT	wind turbine
SOC	state-of-charge
CRR	carbon reduction rate

Indices and sets

t, τ	indexes of time ($t, \tau \in \{1, \ldots, T\}$)
i, j	indexes of microgrids ($i, j \in \{1, \ldots, M\}$)
s	index of storage ($s \in \{ES, HS\}$)
$(\hat{\bullet})$	index of variables in the intra-day phase
$(\tilde{\bullet})$	index of reference values from the day-ahead phase
$\mathcal{M}/\mathcal{T}/\mathcal{S}$	sets of microgrids/time/storage
$\mathcal{H}_t$	set of optimization horizon in time slot t

Parameters

$\eta_i^{e,chp}/\eta_i^{h,chp}$	efficiencies of electricity/heat production for the CHP of microgrid i
$P_{i,\max}^{g,chp}/P_{i,\max}^{g,gb}$	maximum gas consumption for the CHP/GB of microgrid i (kW)
$P_i^{u,chp}/P_i^{d,chp}$	upper/lower bounds of ramp rate limit for the CHP of microgrid i (kW/h)
η_i^{gb}/η_i^{hp}	efficiencies of heat production for the GB/HP of microgrid i
$P_{i,\max}^{e,hp}$	maximum electricity consumption for the HP of microgrid i in each time slot (kW)
$\eta_i^{s,c}/\eta_i^{s,d}$	charging/discharging efficiencies for the storage s of microgrid i
$P_{i,\max}^{s,ch}/P_{i,\max}^{s,dch}$	maximum charging/discharging rates for the storage s of microgrid i (kW)
C_i^s	capacity for the storage s of microgrid i (kWh)
$S^{s,\max}/S^{s,\min}$	maximum/minimum SOCs for the storage s of microgrid i
$\eta_{t,i}$	wind power generation per kW for the WT of microgrid i in time slot t
$P_{i,\max}^{grid}/P_{i,\max}^{gas}$	maximum amounts of electricity/gas that microgrid i can purchase from the utilities in time slot t (kW)
$\overline{P}_{t,i}^{e,l,\max}/\overline{P}_{t,i}^{e,l,\min}$	upper/lower bounds of electricity load elasticity for microgrid i in time slot t (kW)
$\overline{P}_{t,i}^{h,l,\max}/\overline{P}_{t,i}^{h,l,\min}$	upper/lower bounds of heat load elasticity for microgrid i in time slot t (kW)
CE_i^{max}	upper bound of carbon emissions for microgrid i in each day (kg)
λ_i^{CRR}	CRR of microgrid i
em^{grid}/em_i^{gas}	carbon emission rates associated with electricity/gas purchased from the utilities (kg CO_2/kWh)
$em_i^{es}/em_i^{hs}/em_i^{hp}$	carbon emission rates for ESs/HSs/HPs (kg CO_2/kWh)
$p_{t,i}^{e,p}/p_{t,i}^{h,p}$	preferred electricity and gas consumption for microgrid i in time slot t (kW)
$\lambda_t^{grid}/\lambda^{gas}$	electricity/gas prices in time slot t (\$/kW)
λ^c	carbon emission prices (\$/ton CO_2)
λ_i^{load}	unit cost of the deviation from the preferred loads for microgrid i (\$/kW)
$\Delta\hat{P}_{t,i}^{e,a}/\Delta\hat{P}_{t,i}^{h,a}$	deviations from day-ahead forecast values for electricity/heat of microgrid i in time slot t (kW)

Variables

$P_{t,i}^{e,chp}/P_{t,i}^{h,chp}/P_{t,i}^{g,chp}$	electricity production/heat production/gas consumption for the CHP of microgrid i in time slot t (kW)
$P_{t,i}^{h,gb}/P_{t,i}^{g,gb}$	heat production/gas consumption for the GB of microgrid i in time slot t (kW)
$P_{t,i}^{e,hp}/P_{t,i}^{h,hp}$	electricity consumption/heat production for the HP of microgrid i in time slot t (kW)
$E_{t,i}^s$	the amount of stored energy for the storage s of microgrid i in time slot t (kWh)
$P_{t,i}^{s,ch}/P_{t,i}^{s,dch}$	charging/discharging rates for the storage s of microgrid i in time slot t (kW)
$u_{t,i}^{s,ch}/u_{t,i}^{s,dch}$	binary variables indicated charging/discharging state for the storage s of microgrid i in time slot t
$P_{t,i}^{wind}$	scheduled wind power of microgrid i in time slot t (kW)
$P_{t,i}^{grid}/P_{t,i}^{gas}$	the amounts of electricity/gas that microgrid i buys from the utilities in time slot t (kW)
$\overline{P}_{t,i}^{e,l}/\overline{P}_{t,i}^{h,l}$	the amounts of electricity/heat loads adjusted in time slot t (kW)
$P_{t,i}^j$	the amount of electricity that microgrid i receives from microgrid j in time slot t (kW)

multi-follower bi-level optimization framework is proposed in Ref. [10], which minimizes the total operation costs of energy hubs and a distribution network. In Ref. [11], a distributed energy sharing strategy is proposed for multi-energy complementary microgrids considering integrated demand responses. These study demonstrates that it is feasible to consider the coordination and electricity sharing between microgrids in an MMG network, while maintain the network stabilization. However, these study [9–11] only consider the economic scheduling of MMG networks but lack consideration of carbon emissions, so their scheduling results may be environmentally unfriendly or even violate some emission regulations.

Some existing studies have addressed both economic and environmental issues in energy management. These studies can be categorized into two types: independent operation [12–17] and coordinated operation [18–21]. In the research of independent operation, it is assumed that an energy system independently makes local decisions. The low carbon transportation problems are studied in Refs. [12,13], in which the optimal electric vehicle charging strategies are obtained considering the emissions from charging demands. In Refs. [14,15], the potential of hydrogen-powered fuel cell vehicles to reduce greenhouse emissions is studied. In Ref. [16], an optimal power scheduling model for a microgrid is developed, minimizing operation costs and carbon emissions. Optimal design and scheduling of a multi-energy microgrid considering carbon reduction targets are presented in Ref. [17], in which the impact of different carbon reduction targets is demonstrated. In these studies, the coordination between multiple systems is not investigated, limiting the flexibility of a single local system.

In the research of coordinated operation, it is considered that multiple systems coordinate with each other via local energy trading and sharing schemes. In Ref. [18], a peer-to-peer energy and carbon allowance trading framework is proposed for microgrids and implemented on a blockchain platform. A bilevel model of the multi-microgrid system is proposed in Ref. [19], in which energy costs and carbon emissions are minimized. In Ref. [20], a carbon emission flow model associated with energy delivery and conversion processes in multi-energy systems is formulated, and the carbon emission flow calculation procedure is provided. An economic dispatch model for district energy systems consisting of electricity and natural gas networks is formulated in Ref. [21], which achieves an optimized balance between operation costs and carbon emissions. However, the above listed researches have not studied the impact of electricity sharing on the energy management strategy for MMG networks under carbon emission limitations. In addition, most of the existing studies, e.g., Refs. [18–21], only focus on day-ahead scheduling. In fact, the forecast errors of RES generation and load demands will cause real-time deviations from day-ahead markets, so it is possible that the day-ahead scheduling results will violate carbon emission limitations and operation constraints in the intra-day phase.

In view of the above underexplored issues, this paper proposes an optimal energy management strategy for MMG networks, considering both economic and environmental aspects as well as dealing with RES and load variations. Specifically, the proposed strategy includes two phases: day-ahead and intra-day phases. In the day-ahead phase, microgrids operate in a distributed manner and the amount of shared electricity will be determined based on the forecast values of RES generation and load demands. Microgrids submit the preferred demand information to the aggregator at the beginning of the day-ahead scheduling phase. The aggregator, as a manager of the MMG network, determines the energy scheduling for each microgrid considering integrated demand response. In the intra-day phase, the reference values for energy rescheduling are derived from the day-ahead scheduling results. The intra-day rescheduling is implemented using the rolling horizon method [22], which has been demonstrated the feasibility and effectiveness of dealing with the forecast errors in many practical systems, such as electric vehicle charging stations [23], energy hubs [24], and microgrids [25]. The proposed energy management strategy is designed to achieve the minimum operation costs under the carbon emission limitations.

The main features comparison between our paper and related papers is presented in Table 1. As shown in Table 1, this study is an extension of current research on MMG networks. The contributions of this paper are as follows:

1. We propose an optimal energy management strategy for an MMG network to minimize operation costs, considering electricity sharing between microgrids and carbon emission limitations. The aforementioned two aspects have not been fully considered in previous studies on the MMG network, e.g., Refs. [12–17] have not considered the coordination between microgrids, and [9–11] have not considered carbon emission limitations.
2. We propose that the energy management strategy is composed of two phases, including a day-ahead scheduling phase and an intra-day rescheduling phase, to deal with the forecast errors of renewable energy generation and load demands, while preserving the privacy of each microgrid. Existing research on the MMG network, e.g., Refs. [18–21], only focus on the day-ahead scheduling.

The remainder of this paper is organized in the following manner. Section II presents the problem description. In Section III, we formulate the system model of an MMG network. Section IV provides the mathematical formulation of the proposed energy management strategy. Section V presents the simulation cases to demonstrate the effectiveness of the proposed strategy. Finally, we conclude this paper in Section VI.

2. System model

In this section, the modeling of an MMG network and various energy devices in microgrids is presented, followed by the description of integrated demand response, carbon emission limitations, and power balance.

2.1. MMG network

We consider a network of M multi-energy microgrids $\mathcal{M} = \{1, \ldots, M\}$ with three types of energy: electricity, gas, and heat. Each microgrid in the MMG network is indexed by $i \in \mathcal{M}$. Fig. 1 illustrates the basic structure of the MMG network composed of three interconnected microgrids. The bidirectional electricity flows between different microgrids are achieved through power lines, while information exchange can be implemented by wireless communication networks. Several types of energy devices are considered, including combined heat and power units (CHPs), gas boilers (GBs), heat pumps (HPs), electric storages (ESs), and heat storages (HSs). Wind turbines (WTs) are introduced as a type of RES. We consider that the wind curtailment can be reduced through two different ways. On the one hand, the redundant wind power can be converted to heat energy through HPs for usage or storage. In this way, the redundant wind power can be used to meet the local heat demands. On the other hand, the redundant wind power of a microgrid can be transmitted via power lines to microgrids that are deficient in electricity. It is based on the fact that different microgrids have diverse RES generation and load demands. Thus, we consider the electricity sharing among microgrids.

Each microgrid is connected to the main power grid and gas network, and is supervised by an aggregator. The aggregator is also responsible for electricity sharing management and operation security within the network. We consider that the scheduling horizon of one day is denoted as $\mathcal{T} = \{1, \ldots, T\}$, where $T = 24$.

To implement the energy management in the MMG network,

Table 1
Feature comparison between this paper and related works (Y: YES; N: NO).

Features	[3]	[4]	[5]	[9]	[10]	[11]	[12]	[17]	[18]	[19]	[20]	[21]	This study
Energy sharing	Y	Y	Y	Y	Y	Y	N	N	Y	Y	Y	N	Y
Multi-energy	N	N	N	Y	Y	Y	N	Y	N	Y	Y	Y	Y
Carbon emissions	N	N	N	N	N	N	Y	Y	Y	Y	Y	Y	Y
Forecast errors	Y	N	Y	Y	N	Y	N	Y	N	N	N	N	Y
Demand response	N	Y	Y	N	N	Y	N	N	N	N	N	Y	Y
Decentralization	Y	Y	Y	Y	N	Y	N	N	Y	N	N	N	Y

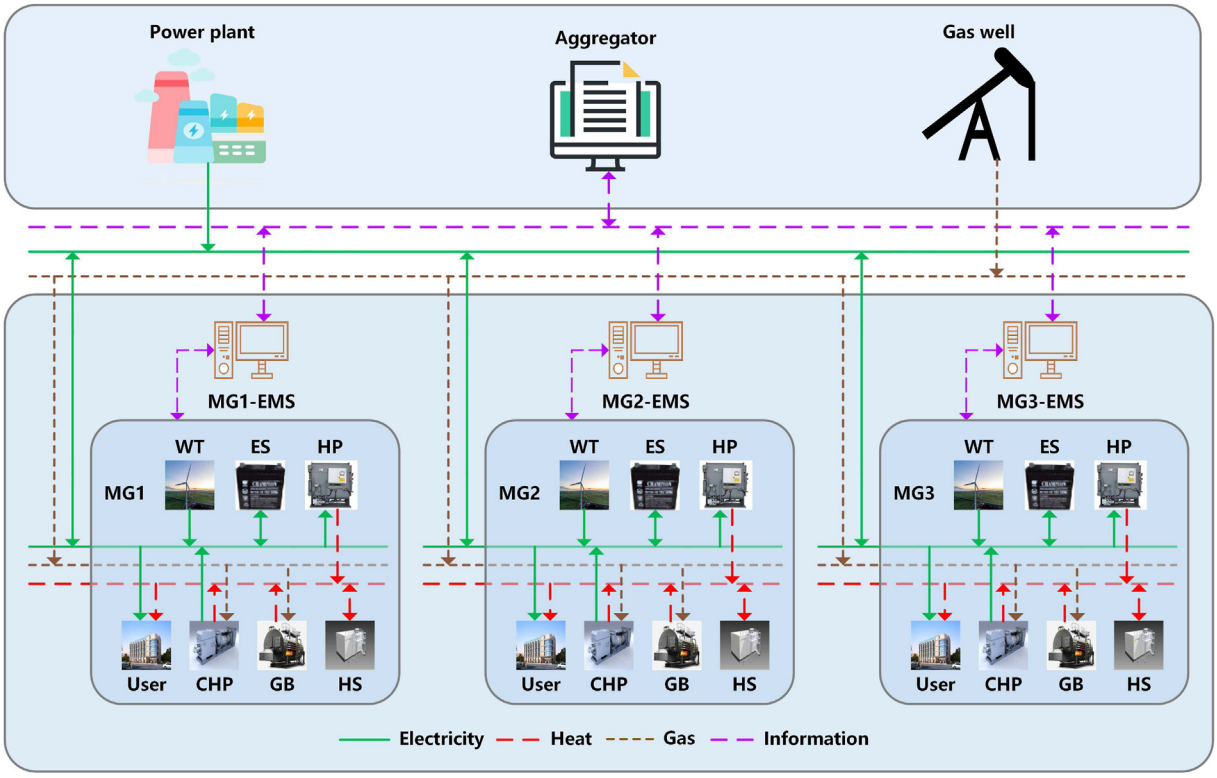

Fig. 1. Basic structure of an MMG network (MG: Microgrid; EMS: Energy management system).

each microgrid should be able to: (1) meter and forecast the renewable energy generation and load demands; (2) solve its local optimization problem; (3) communicate with other microgrids; (4) transmit electricity to other microgrids. All of these are implementable for microgrids by employing advanced computing, communication, and electricity transmission technologies.

2.2. Multi-energy microgrid model

Fig. 2 shows the structure of a multi-energy microgrid and energy flow directions. The detailed model of each device is as follows.

2.2.1. CHP

Energy conversion of a CHP, which burns gas to generate heat and electricity, is described as:

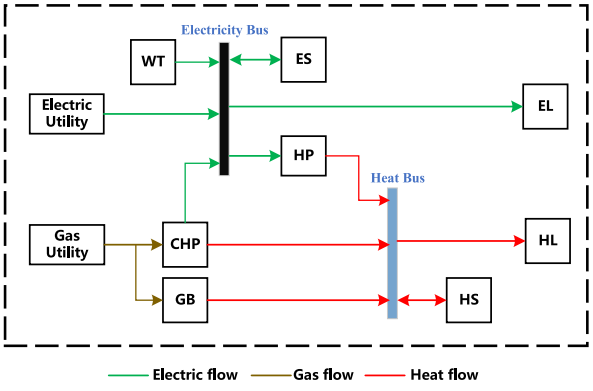

Fig. 2. Structure of a multi-energy microgrid with energy flow directions.

$$P_{t,i}^{e,chp} = \eta_i^{e,chp} P_{t,i}^{g,chp}, \quad \forall t \in \mathcal{T}, \forall i \in \mathcal{M} \tag{1}$$

$$P_{t,i}^{h,chp} = \eta_i^{h,chp} P_{t,i}^{g,chp}, \quad \forall t \in \mathcal{T}, \forall i \in \mathcal{M} \tag{2}$$

where $P_{t,i}^{e,chp}$, $P_{t,i}^{h,chp}$, and $P_{t,i}^{g,chp}$ denote electricity production, heat production, and gas consumption of the CHP of microgrid i in time slot t, respectively; $\eta_i^{e,chp}$ and $\eta_i^{h,chp}$ represent the efficiencies of electricity and heat production, respectively. Moreover, CHPs satisfy the gas consumption bounds and ramp rate limits, which are described by:

$$0 \le P_{t,i}^{g,chp} \le P_{i,\max}^{g,chp}, \quad \forall t \in \mathcal{T}, \forall i \in \mathcal{M} \tag{3}$$

$$P_i^{d,chp} \le P_{t,i}^{g,chp} - P_{t-1,i}^{g,chp} \le P_i^{u,chp}, \ \forall t \in \mathcal{T}, \forall i \in \mathcal{M} \tag{4}$$

where $P_{i,\max}^{g,chp}$ denotes the maximum gas consumption of the CHP; $P_i^{u,chp}$ and $P_i^{d,chp}$ are the upper and lower bounds for ramp rate limits, respectively.

2.2.2. GB

Energy conversion of a GB, which consumes gas to produce heat, is described by:

$$P_{t,i}^{h,gb} = \eta_i^{gb} P_{t,i}^{g,gb}, \quad \forall t \in \mathcal{T}, \forall i \in \mathcal{M} \tag{5}$$

where $P_{t,i}^{h,gb}$ and $P_{t,i}^{g,gb}$ are heat production and gas consumption of the GB of microgrid i in time slot t, respectively; η_i^{gb} represents the efficiency of heat production of the GB. The gas consumption

bounds for the GB are provided by:

$$0 \le P_{t,i}^{g,gb} \le P_{i,\max}^{g,gb}, \quad \forall t \in \mathcal{T}, \forall i \in \mathcal{M} \tag{6}$$

where $P_{i,\max}^{g,gb}$ denotes the maximum gas consumption.

2.2.3. HP

Energy conversion and electricity consumption constraints of an HP are given by:

$$P_{t,i}^{h,hp} = \eta_i^{hp} P_{t,i}^{e,hp}, \quad \forall t \in \mathcal{T}, \forall i \in \mathcal{M} \tag{7}$$

$$0 \le P_{t,i}^{e,hp} \le P_{i,\max}^{e,hp}, \quad \forall t \in \mathcal{T}, \forall i \in \mathcal{M} \tag{8}$$

where $P_{t,i}^{e,hp}$ and $P_{t,i}^{h,hp}$ are electricity consumption and heat production of the HP, respectively; η_i^{hp} is the energy conversion efficiency of the HP; $P_{i,\max}^{e,hp}$ denotes the maximum electricity consumption of the HP.

2.2.4. ES and HS

Due to the similar mathematical model of an ES and an HS, we define $\mathcal{S} = \{ES, HS\}$ as the set of these two types of storage. The energy storage dynamics of microgrid i is shown as:

$$E_{t,i}^{s} = E_{t-1,i}^{s} + \eta_i^{s,c} P_{t,i}^{s,ch} \Delta t - (1/\eta_i^{s,d}) P_{t,i}^{s,dch} \Delta t, \quad \forall t \in \mathcal{T}, \forall i \in \mathcal{M}, \forall s \in \mathcal{S} \tag{9}$$

where $E_{t,i}^{s}$, $P_{t,i}^{s,ch}$ and $P_{t,i}^{s,dch}$ denote the amount of stored energy, charging rate, and discharging rate for the storage $s \in \mathcal{S}$ of microgrid i in time slot t, respectively; $\eta_i^{s,c}$ and $\eta_i^{s,d}$ denote the charging and discharging efficiencies of storage s. As charging and discharging cannot happen at the same time, we introduce two binary variables $u_{t,i}^{s,ch}$ and $u_{t,i}^{s,dch}$ [26], and impose the following constraints:

$$0 \le P_{t,i}^{s,ch} \le u_{t,i}^{s,ch} P_{i,\max}^{s,ch}, \quad \forall t \in \mathcal{T}, \forall i \in \mathcal{M}, \forall s \in \mathcal{S} \tag{10}$$

$$0 \le P_{t,i}^{s,dch} \le u_{t,i}^{s,dch} P_{i,\max}^{s,dch}, \quad \forall t \in \mathcal{T}, \forall i \in \mathcal{M}, \forall s \in \mathcal{S} \tag{11}$$

$$0 \le u_{t,i}^{s,ch} + u_{t,i}^{s,dch} \le 1, \quad u_{t,i}^{s,ch}, u_{t,i}^{s,dch} \in \{0,1\} \quad \forall t \in \mathcal{T}, \forall i \in \mathcal{M}, \forall s \in \mathcal{S} \tag{12}$$

where $P_{i,\max}^{s,ch}$ and $P_{i,\max}^{s,dch}$ are the maximum charging and discharging rates of storage s, respectively. The amount of stored energy for the storage s should satisfy the following constraints:

$$S^{s,\min} C_i^s \le E_{t,i}^s \le S^{s,\min} C_i^s, \quad \forall t \in \mathcal{T}, \forall i \in \mathcal{M}, \forall s \in \mathcal{S} \tag{13}$$

$$E_{1,i}^s = E_{T,i}^s, \quad \forall i \in \mathcal{M}, \forall s \in \mathcal{S} \tag{14}$$

where C_i^s, $S^{s,\max}$, and $S^{s,\min}$ represent the storage capacity, maximum state-of-charge (SOC), and minimum SOC, respectively. Constraint (14) denotes that the stored energy of storage s at the beginning and end of the scheduling horizon would be the same.

2.2.5. WT

Let G_i denote the generation capacity for the WT of microgrid i. The actual scheduling of wind power is subject to:

$$0 \le P_{t,i}^{wind} \le \eta_{t,i} G_i, \quad \forall t \in \mathcal{T}, \forall i \in \mathcal{M} \tag{15}$$

where $\eta_{t,i}$ represents wind power generation per kW.

2.3. Outer energy networks

Let $P_{t,i}^{grid}$ and $P_{t,i}^{gas}$ represent the amounts of electricity and gas that microgrid i buys from the outer networks in time slot t. They are subjected to the following constraints:

$$0 \le P_{t,i}^{grid} \le P_{i,\max}^{grid}, \quad \forall t \in \mathcal{T}, \forall i \in \mathcal{M} \tag{16}$$

$$0 \le P_{t,i}^{gas} \le P_{i,\max}^{gas}, \quad \forall t \in \mathcal{T}, \forall i \in \mathcal{M} \tag{17}$$

where $P_{i,\max}^{grid}$ and $P_{i,\max}^{gas}$ denote the maximum amounts of electricity and gas that microgrid i can purchase from the electricity and gas utilities, respectively.

2.4. Integrated demand response

Integrated demand response is implemented for electricity and heat loads in the day-ahead phase. We introduce two variables $\overline{P}_{t,i}^{e,l}$ and $\overline{P}_{t,i}^{h,l}$ to describe the amounts of electricity and heat loads that can be adjusted, respectively. They are subjected to the following constraints:

$$\overline{P}_{t,i}^{e,l,\min} \le \overline{P}_{t,i}^{e,l} \le \overline{P}_{t,i}^{e,l,\max}, \quad \forall t \in \mathcal{T}, \forall i \in \mathcal{M} \tag{18}$$

$$\overline{P}_{t,i}^{h,l,\min} \le \overline{P}_{t,i}^{h,l} \le \overline{P}_{t,i}^{h,l,\max}, \quad \forall t \in \mathcal{T}, \forall i \in \mathcal{M} \tag{19}$$

$$\sum_{t \in \mathcal{T}} \overline{P}_{t,i}^{e,l} = 0, \quad \forall i \in \mathcal{M} \tag{20}$$

$$\sum_{t \in \mathcal{T}} \overline{P}_{t,i}^{h,l} = 0, \quad \forall i \in \mathcal{M} \tag{21}$$

where $\overline{P}_{t,i}^{e,l,\max}$ and $\overline{P}_{t,i}^{e,l,\min}$ provide the upper and lower bounds of electricity elasticity for microgrid i in time slot t, respectively. For the heat elasticity, $\overline{P}_{t,i}^{h,l,\max}$ and $\overline{P}_{t,i}^{h,l,\min}$ have similar definitions. Constraints (20) and (21) denote that the total electricity and heat requirements in one day remain unchanged.

2.5. Carbon emission limitations

For the sake of environmental protection, the carbon emissions associated with consuming gas and electricity are restricted. We denote the total carbon emissions of microgrid i in the whole scheduling horizon as CE_i. Carbon emission rates of different energy devices are defined as em_i^{gas} for CHPs and GBs, em_i^{es} for ESs, em_i^{hs} for HSs, and em_i^{hp} for HPs. The carbon emission rate associated with electricity purchased from the electric utility is denoted as em^{grid}. The total amount of carbon emissions for microgrid i is written as (22). Constraint (23) denotes the carbon emission limitations.

$$CE_i = \sum_{t\in\mathcal{T}} \begin{pmatrix} em_i^{gas}\left(P_{t,i}^{g,chp} + P_{t,i}^{g,gb}\right) + \\ em_i^{es}\left(P_{t,i}^{es,ch} + P_{t,i}^{es,dch}\right) + \\ em_i^{hs}\left(P_{t,i}^{hs,ch} + P_{t,i}^{hs,dch}\right) + \\ em_i^{hp}P_{t,i}^{e,hp} + em^{grid}P_{t,i}^{grid} \end{pmatrix}, \quad \forall i\in\mathcal{M} \tag{22}$$

$$CE_i \le \left(1-\lambda_i^{CRR}\right)CE_i^{\max}, \quad \forall i\in\mathcal{M} \tag{23}$$

where $CE_i^{\max}$ represents the upper bound of carbon emissions of microgrid i; λ_i^{CRR} denotes the carbon reduction rate (CRR) of microgrid i.

2.6. Power balance

We consider that each microgrid is willing to share electricity with other interconnected microgrids to reduce system-wide operation costs. Let $P_{t,i}^{j}>0$ denote the amount of electricity that microgrid i receives from microgrid $j, j\in\mathcal{M}\backslash i$ in time slot t, while $P_{t,i}^{j}<0$ indicates that microgrid i sends electricity to microgrid j. We have $P_{t,i}^{j} + P_{t,j}^{i} = 0$. The power balance equations for electricity, heat, and gas in the MMG network are described by:

$$\begin{aligned} &P_{t,i}^{grid} + P_{t,i}^{wind} + P_{t,i}^{e,chp} + P_{t,i}^{es,dch} + \sum_{j\in\mathcal{M}\backslash i} P_{t,i}^{j} \\ &\quad = P_{t,i}^{e,p} + \overline{P}_{t,i}^{e,l} + P_{t,i}^{es,ch} + P_{t,i}^{e,hp}, \quad \forall t\in\mathcal{T}, \forall i\in\mathcal{M} \end{aligned} \tag{24}$$

$$\begin{aligned} &P_{t,i}^{h,chp} + P_{t,i}^{h,gb} + P_{t,i}^{h,hp} + P_{t,i}^{hs,dch} \\ &\quad = P_{t,i}^{h,p} + \overline{P}_{t,i}^{h,l} + P_{t,i}^{hs,ch}, \quad \forall t\in\mathcal{T}, \forall i\in\mathcal{M} \end{aligned} \tag{25}$$

$$P_{t,i}^{gas} = P_{t,i}^{g,chp} + P_{t,i}^{g,gb}, \quad \forall t\in\mathcal{T}, \forall i\in\mathcal{M} \tag{26}$$

where $P_{t,i}^{e,p}$ and $P_{t,i}^{h,p}$ denote the preferred electricity and gas consumption for microgrid i in time slot t.

3. Energy management strategy for MMG networks

In this section, we present the formulation of the proposed energy management strategy. We first briefly present the strategy structure and then describe the detailed strategies for the day-ahead scheduling phase and the intra-day rescheduling phase.

3.1. Strategy structure

The energy management strategy for MMG networks consists of a day-ahead scheduling phase and an intra-day rescheduling phase. The two-phase structure is for coping with the uncertainties of RES generation and load demands. The proposed strategy has three major superiorities: 1) preserving the privacy of each microgrid; 2) reducing carbon emissions and wind power curtailment; and 3) stabilizing the operation of the electricity network, gas network, and energy devices. In the day-ahead scheduling phase, the optimal energy scheduling plans for the next day are obtained for minimizing system-wide costs. In the intra-day rescheduling phase, each microgrid adapts to its RES and load deviations by rescheduling the energy devices hour-by-hour.

- In the day-ahead scheduling phase, the operation constraints and carbon emission limitations will be taken into account with the predicted values of wind power generation and loads. Under a distributed electricity sharing manner, four scheduling plans will be determined for all microgrids in the MMG network: 1) the amounts of electricity and gas purchased from the utilities; 2) the operation plans of energy devices, 3) the amounts of electricity shared between interconnected microgrids; 4) the adjusted amounts of electricity and heat loads. These scheduling results would be used in the intra-day rescheduling problem as the reference parameters.
- In the intra-day rescheduling phase, the operation of energy devices and energy procurement are rescheduled based on the actual amounts of RES generation and load demands. To reduce the communication and computation burden [5], the amounts of electricity shared among microgrids will be consistent with the day-ahead scheduling results. In order to meet the real demands of microgrids, integrated demand response is not considered in the intra-day phase. Besides the operation costs, the penalty costs induced by the adjustment of energy devices and energy procurement are considered. A rolling horizon optimization strategy is employed for rescheduling optimization.

3.2. Day-ahead scheduling phase

3.2.1. Objective function

The objective of the day-ahead scheduling phase is to minimize the social operation cost of the MMG network based on the predicted values of wind power generation and electricity and heat loads, denoted as:

$$\min_{\Pi} \sum_{i\in\mathcal{M}} \left\{F_i^{grid} + F_i^{gas} + F_i^{load} + F_i^{carbon}\right\} \tag{27}$$

$$F_i^{grid} = \sum_{t\in\mathcal{T}} \lambda_t^{grid} P_{t,i}^{grid} \Delta t \tag{28}$$

$$F_i^{gas} = \sum_{t\in\mathcal{T}} \lambda^{gas} P_{t,i}^{gas} \Delta t \tag{29}$$

$$F_i^{load} = \sum_{t\in\mathcal{T}} \lambda_i^{load} \left(\left(\overline{P}_{t,i}^{e,l}\right)^2 + \left(\overline{P}_{t,i}^{h,l}\right)^2 \right) \Delta t \tag{30}$$

$$F_i^{carbon} = \lambda^{c} CE_i \Delta t \tag{31}$$

where decision variables are $\Pi = \{P_{t,i}^{grid}, P_{t,i}^{gas}, P_{t,i}^{g,chp}, P_{t,i}^{g,gb}, P_{t,i}^{e,hp}, P_{t,i}^{s,ch}, P_{t,i}^{s,dch}, u_{t,i}^{s,ch}, u_{t,i}^{s,dch}, P_{t,i}^{j}, \overline{P}_{t,i}^{e,l}, \overline{P}_{t,i}^{h,l} | t\in\mathcal{T}, i\in\mathcal{M}, s\in\mathcal{S}, j\in\mathcal{M}\backslash i\}$. The social operation cost is the sum of four terms: electricity purchase cost F_i^{grid}, gas purchase cost F_i^{gas}, demand adjustment cost F_i^{load}, and carbon emission cost F_i^{carbon}, as shown by (28)-(31). λ_t^{grid}, λ^{gas}, and λ^{c} denote the electricity, gas, and carbon emission prices, respectively, while λ_i^{load} is used to quantify the unit cost of the deviation from the preferred loads for microgrid i.

3.2.2. Constraints

To guarantee the secure operation of the MMG network, the following constraints should be met:

(1) Energy device constraints for each microgrid i including CHP constraints (1)–(4), GB constraints (5)–(6), HP constraints (7)–(8), storage constraints (9)–(14), and WT constraint (15);
(2) Outer network constraints for electricity and gas purchase (16)–(17);
(3) Integrated demand response constraints for electricity and heat loads (18)–(21);
(4) Carbon emission limitations (22)–(23);
(5) Energy balance constraints for electricity, heat, and gas (24)–(26).

The optimization problem of the day-ahead scheduling phase is a mixed integer linear programming (MILP) problem. We develop a distributed algorithm to solve this problem, which will be described in detail later. After the optimization, the results of decision variables Π will be used as the referenced values for the intra-day rescheduling. Here, we define $P^{e,a}_{t,i}$ and $P^{h,a}_{t,i}$ as the scheduled results of electricity and heat loads for microgrid i in time slot t after the day-ahead scheduling phase, where $P^{e,a}_{t,i} = P^{e,p}_{t,i} + \overline{P}^{e,l}_{t,i}$ and $P^{h,a}_{t,i} = P^{h,p}_{t,i} + \overline{P}^{h,l}_{t,i}$. $P^{e,a}_{t,i}$ and $P^{h,a}_{t,i}$ are parameters in the intra-day rescheduling problem.

3.3. Intra-day rescheduling phase

3.3.1. Objective function

The objective of microgrid i in the intra-day rescheduling phase is to minimize the weighted sum of operation costs and penalty costs induced by the deviation from the day-ahead scheduling results, as shown by:

$$\min_{\Gamma_t} \left\{ \theta\left(\hat{F}^{grid}_{t,i} + \hat{F}^{gas}_{t,i} + \hat{F}^{carbon}_{t,i}\right) + (1-\theta)\hat{F}^{dev}_{t,i} \right\} \tag{32}$$

$$\hat{F}^{dev}_{t,i} = \tag{33}$$

$$\sum_{\tau\in\mathcal{H}_t} \lambda^{dev} \left[\begin{array}{c} \left(\hat{P}^{g,chp}_{\tau,i} - \tilde{P}^{g,chp}_{\tau,i}\right)^2 + \left(\hat{P}^{g,gb}_{\tau,i} - \tilde{P}^{g,gb}_{\tau,i}\right)^2 + \\ \left(\hat{P}^{e,hp}_{\tau,i} - \tilde{P}^{e,hp}_{\tau,i}\right)^2 + \left(\hat{P}^{s,ch}_{\tau,i} - \tilde{P}^{s,ch}_{\tau,i}\right)^2 + \\ \left(\hat{P}^{s,dch}_{\tau,i} - \tilde{P}^{s,dch}_{\tau,i}\right)^2 + \left(\hat{P}^{grid}_{\tau,i} - \tilde{P}^{grid}_{\tau,i}\right)^2 + \\ \left(\hat{P}^{gas}_{\tau,i} - \tilde{P}^{gas}_{\tau,i}\right)^2 \end{array} \right]$$

where decision variables are $\Gamma_t = \{\hat{P}^{grid}_{\tau,i}, \hat{P}^{gas}_{\tau,i}, \hat{P}^{g,chp}_{\tau,i}, \hat{P}^{g,gb}_{\tau,i}, \hat{P}^{e,hp}_{\tau,i}, \hat{P}^{s,ch}_{\tau,i}, \hat{P}^{s,dch}_{\tau,i}, \hat{u}^{s,ch}_{\tau,i}, \hat{u}^{s,dch}_{\tau,i} | \tau \in \mathcal{H}_t, i \in \mathcal{M}, s \in \mathcal{S}, j \in \mathcal{M}\backslash i\}$; λ^{dev} denotes the unit penalty cost for the deviation from the day-ahead schedules. Note that $(\hat{\bullet})$ denotes the variables in the intra-day phase and $(\tilde{\bullet})$ denotes the reference values from the day-ahead phase. The intra-day rescheduling problem is solved using a rolling horizon strategy, in which the optimization horizon in time slot t is $\mathcal{H}_t = \{t, \ldots, T\}$. $0 \le \theta \le 1$ is the weight parameter that adjusts the trade-off between operation costs $(\hat{F}^{grid}_{t,i} + \hat{F}^{gas}_{t,i} + \hat{F}^{carbon}_{t,i})$ and penalty costs $\hat{F}^{dev}_{t,i}$. If $\theta = 1$, then microgrid i is interested only in minimizing the operation costs. If $\theta = 0$, then microgrid i focuses only on minimizing the penalty costs, i.e., making the intra-day operation follow the day-ahead schedule as much as possible. The objective function in the intra-day phase uses the weighted sum of operation costs and penalty costs to identify all the points on the Pareto boundary [27], which will be discussed in Section 4.

3.3.2. Constraints

In the intra-day phase, the amounts of electricity exchanged between different microgrids are consistent with the day-ahead scheduling results, and integrated demand response is not taken into account. The energy device constraints, outer network constraints, and carbon emission limitations are similar to those in the day-ahead scheduling model, i.e. (1)–(15), (16)–(17), and (22)–(23). The different parts of the intra-day rescheduling phase are shown below:

(1) Power balance constraints:

$$\begin{aligned} &\hat{P}^{grid}_{\tau,i} + \hat{P}^{wind}_{\tau,i} + \hat{P}^{e,chp}_{\tau,i} + \hat{P}^{es,dch}_{\tau,i} + \sum_{j\in\mathcal{M}\backslash i} \tilde{P}^{j}_{\tau,i} \\ &\quad = \tilde{P}^{e,a}_{\tau,i} + \Delta\hat{P}^{e}_{\tau,i} + \hat{P}^{es,ch}_{\tau,i} + \hat{P}^{e,hp}_{\tau,i}, \quad \forall \tau \in \mathcal{H}_t, \forall i \in \mathcal{M} \end{aligned} \tag{34}$$

$$\begin{aligned} &\hat{P}^{h,chp}_{\tau,i} + \hat{P}^{h,gb}_{\tau,i} + \hat{P}^{h,hp}_{\tau,i} + \hat{P}^{hs,dch}_{\tau,i} \\ &\quad = \tilde{P}^{h,a}_{\tau,i} + \Delta\hat{P}^{h}_{\tau,i} + \hat{P}^{hs,ch}_{\tau,i}, \quad \forall \tau \in \mathcal{H}_t, \forall i \in \mathcal{M} \end{aligned} \tag{35}$$

$$\hat{P}^{gas}_{\tau,i} = \hat{P}^{g,chp}_{\tau,i} + \hat{P}^{g,gb}_{\tau,i}, \quad \forall \tau \in \mathcal{H}_t, \forall i \in \mathcal{M} \tag{36}$$

where $\Delta\hat{P}^{e,a}_{t,i}$ and $\Delta\hat{P}^{h,a}_{t,i}$ are the actual deviation from day-ahead forecast values of electricity and heat loads, measured locally in time slot t, respectively.

(2) Integrated demand response constraints are eliminated.

The optimization problem in the intra-day rescheduling phase is a mixed integer quadratic programming (MIQP) problem and can be solved locally by the individual microgrid. It is because the problem only involves the local information of a microgrid without the need to interact with other microgrids. In the rolling horizon strategy, the optimization problem in time slot t is based on the actual measurement of wind power generation and load demands in time slot t and their forecast values in the remaining time slots $\{t+1, \ldots, T\}$. For the optimal solution Γ_t, only the solution for the current time slot t is implemented, while the solution for the remaining time slots $\{t+1, \ldots, T\}$ is discarded. When the next time slot $t+1$ arrives, the optimization horizon becomes $\mathcal{H}_{t+1} = \{t+1, \ldots, T\}$. Thus, in the intra-day phase, there are $T = 24$ optimization problems with decreasing sizes of horizons should be solved sequentially.

3.4. Algorithms

Although the day-ahead scheduling problem can be solved with off-the-shelf solvers, the centralized optimization method requires complete information of each microgrid, which may disclose the privacy of microgrids. In this regard, we develop a distributed algorithm based on ADMM [28] for solving the day-ahead scheduling problem (27). To guarantee the convergence of the distributed algorithm, we formulate the day-ahead scheduling problem in a two-block structure [4,28]. Specifically, we introduce auxiliary variables $\overline{P}^{j}_{t,i}, \forall t \in \mathcal{T}, \forall i \in \mathcal{M}, \forall j \in \mathcal{M}\backslash i$ for the energy trading decisions, which satisfy the following constraints:

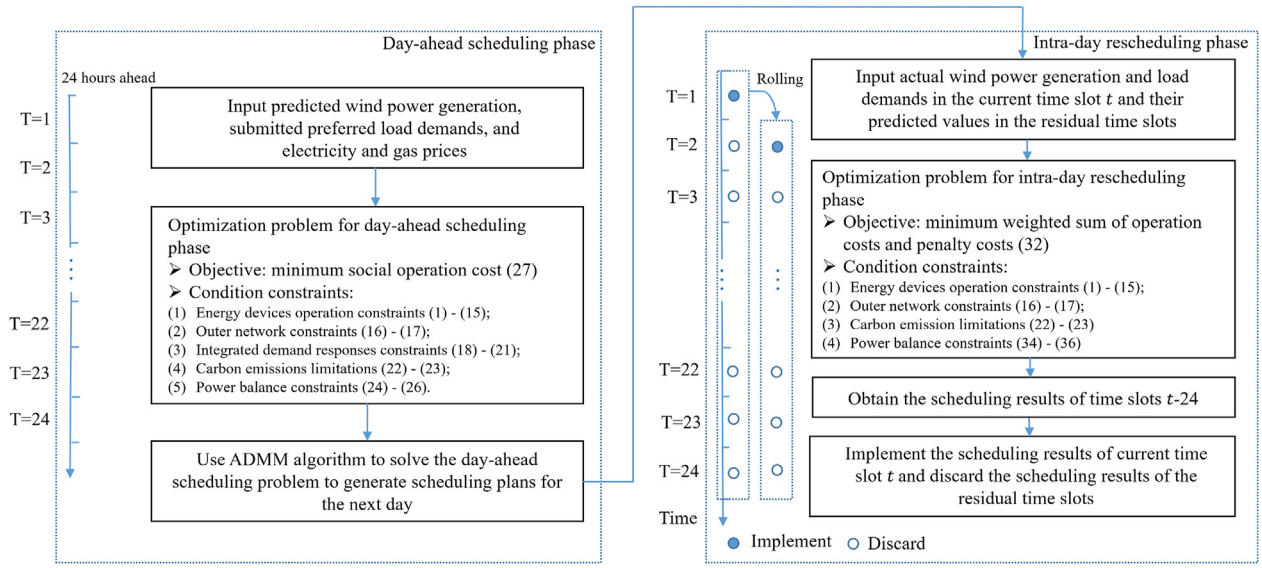

Fig. 3. Implementation of the energy management strategy for MMG networks.

Table 2
MMG network parameters [17,33].

Parameters	Values	Parameters	Values
G_i(kW)	150	$P^{g,gb}_{i,\max}$ (kW)	35
C^{es}_i/C^{hs}_i(kWh)	60/50	$P^{e,hp}_{i,\max}$ (kW)	40
$\eta^{es,d}_i/\eta^{hs,d}_i$	0.95/0.95	$P^{es,ch}_{i,\max}/P^{hs,ch}_{i,\max}$ (kW)	10/18
$\eta^{es,c}_i/\eta^{hs,c}_i$	0.2/0.2	$P^{es,dch}_{i,\max}/P^{hs,dch}_{i,\max}$ (kW)	10/18
$P^{g,chp}_{i,\max}$ (kW)	80	$S^{es}_{\max}/S^{hs}_{\max}$	0.9/0.9
$P^{u,chp}_i/P^{d,chp}_i$(kW)	20/20	$S^{es}_{\min}/S^{hs}_{\min}$	0.2/0.2
em^{gas}_i(kg CO_2/kWh)	0.202	em^{es}_i(kg CO_2/kWh)	0.083
em^{hs}_i(kg CO_2/kWh)	0	em^{hp}_i(kg CO_2/kWh)	0.12
em^{grid}(kg CO_2/kWh)	0.202		

$$\overline{P}^j_{t,i} = P^j_{t,i}, \quad \forall t\in\mathcal{T}, \forall i\in\mathcal{M}, \forall j\in\mathcal{M}\backslash i \tag{37}$$

$$\overline{P}^j_{t,i} + \overline{P}^i_{t,j} = 0, \quad \forall t\in\mathcal{T}, \forall i\in\mathcal{M}, \forall j\in\mathcal{M}\backslash i \tag{38}$$

We define the dual variables $\lambda^t_{i,j}, \forall t\in\mathcal{T}, \forall i\in\mathcal{M}, \forall j\in\mathcal{M}\backslash i$ associated with constraints (38). By this way, we can derive the augmented Lagrangian for the day-ahead scheduling problem (27) as:

$$\mathcal{L} = \sum_{i\in\mathcal{M}} \left[\begin{array}{c} F^{grid}_i + F^{gas}_i + F^{load}_i + F^{carbon}_i + \\ \sum_{j\in\mathcal{M}\backslash i}\sum_{t\in\mathcal{T}} \left(\frac{\rho}{2}\left(\overline{P}^j_{t,i} - P^j_{t,i}\right)^2 + \lambda^t_{i,j}\left(\overline{P}^j_{t,i} - P^j_{t,i}\right)\right) \end{array} \right] \tag{39}$$

where the parameter $\rho > 0$ is the penalty coefficient.

The ADMM-based distributed algorithm consists of three steps. In the first step (**S1**), given the auxiliary variables $\overline{P}^j_{t,i}(k)$ and dual variables $\lambda^t_{i,j}(k)$, each microgrid i solves its local energy scheduling problem:

3.4.1. S1

Local energy scheduling problem:

$$\min_{\Pi_{S1}} \left(F^{grid}_i + F^{gas}_i + F^{load}_i + F^{carbon}_i\right) + \sum_{j\in\mathcal{M}\backslash i}\sum_{t\in\mathcal{T}} \left(\frac{\rho}{2}\left(\overline{P}^j_{t,i}(k) - P^j_{t,i}\right)^2 - \lambda^t_{i,j}(k)P^j_{t,i}\right) \tag{40}$$

subject to (1)–(26). where decision variables are $\Pi_{S1} = \Pi$. Note that problem (40) is an MIQP problem.

Based on the optimal solution $P^j_{t,i}(k+1)$ from the step **S1**, the second step (**S2**) involves updating the auxiliary variables $\overline{P}^j_{t,i}$ by solving the following problem:

3.4.2. S2

Updating auxiliary variables:

$$\min_{\Pi_{S2}} \sum_{i\in\mathcal{M}}\sum_{j\in\mathcal{M}\backslash i}\sum_{t\in\mathcal{T}} \left(\frac{\rho}{2}\left(\overline{P}^j_{t,i} - P^j_{t,i}(k+1)\right)^2 + \lambda^t_{i,j}(k)\overline{P}^j_{t,i}\right) \tag{41}$$

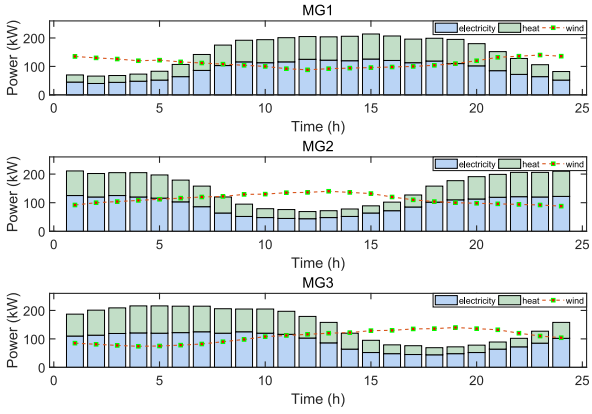

Fig. 4. Electricity loads, heat loads, and wind power generation of the microgrids.

subject to (38).where decision variables are $\Pi_{S2} = \{\overline{P}^j_{t,i} | \forall t \in \mathcal{T}, \forall i \in \mathcal{M}, \forall j \in \mathcal{M}\backslash i\}$. The optimal solution to (41) can be directly given by:

$$\begin{aligned}\overline{P}^j_{t,i}(k+1) &= -\overline{P}^i_{t,j}(k+1) \\ &= \frac{1}{2\rho}\left(\rho\left(P^j_{t,i}(k+1) - P^i_{t,j}(k+1)\right) - \left(\lambda^t_{i,j}(k) - \lambda^t_{j,i}(k)\right)\right)\end{aligned} \tag{42}$$

Based on the results of $P^j_{t,i}(k+1)$ and $\overline{P}^j_{t,i}(k+1)$ solved by the step **S1** and **S2**, the third step (**S3**) involves updating the dual variables $\lambda^t_{i,j}$ as follows:

3.4.3. S3

Updating dual variables:

$$\lambda^t_{i,j}(k+1) = \lambda^t_{i,j}(k) + \rho\left(\overline{P}^j_{t,i}(k+1) - P^j_{t,i}(k+1)\right) \tag{43}$$

The three steps repeat sequentially until the following stop condition is met:

$$\sum_{i \in \mathcal{M}} \sum_{j \in \mathcal{M}\backslash i} \left\| \overline{P}^j_{t,i}(k+1) - P^j_{t,i}(k) \right\| < \epsilon \tag{44}$$

where ϵ is a very small positive constant. Note that the left side of (44) denotes the primal residual of the distributed algorithm.

In these three steps, the cost and constraint information of each microgrid is only used for local optimization problem, protecting the privacy of the microgrids. The convergence of the ADMM-based distributed algorithm and the accuracy of results will be presented in Section 4.

Fig. 3 provides a flowchart illustrating the proposed energy management strategy and the connection between the day-ahead and intra-day phases. Note that the intra-day rescheduling problem (32) is solved locally by each microgrid. Problem (32) and problem (40) are MIQP problems, which can be solved by many exact algorithms, such as the approach proposed in Ref. [29] using a general branch-and-bound framework and the approach in Ref. [30] that combines branch and bound with non-negative least square. In this paper, the MIQP problems are solved by commercial solvers.

4. Simulation cases

In this section, we carry out simulations in different cases to evaluate the performance of the proposed optimal energy management strategy for MMG networks. The simulation cases are implemented in MATLAB. The MILP and MIQP problems are solved by Gurobi [31]. The MMG network configuration is shown in Fig. 1. We consider that each microgrid has the same energy devices and structure. The amount of adjustable electricity and heat loads are set to be $\pm 10\%$ of the submitted preferred consumption values [32]. The upper limits of electricity and gas that each microgrid can purchase from the utilities are set as 1000 kW. The unit cost of deviation from the preferred loads is 0.002 \$/kW [4]. The carbon emission price is 20 \$/*ton* CO_2 [17]. The parameters related to the energy devices and carbon emission rates are tabulated in Table 2. The weight for balancing operation costs and penalty costs in the intra-day phase is $\theta = 0.5$ for all microgrids by default. For each microgrid, we set the CRR is the same in both the day-ahead and intra-day phases. We set that $CE_i^{\max}$ is equal to the total amount of carbon emissions of microgrid i for one day in day-ahead scheduling phase when no carbon emission limitations are taken into account. Thus, $CE_i^{\max}$ denotes the amount of carbon emissions in the case of no emission limitations.

4.1. Basic data

Fig. 4 shows the day-ahead predicted wind power generation and preferred consumption of electricity and gas for the three microgrids. In the experiment, we consider that wind power generation and electricity and gas loads have 10% random disturbances and the random disturbances are added on the day-ahead predicted values as their real values [32]. As observed from Fig. 4, the three microgrids have different time intervals of energy surplus and energy shortage. The electricity prices of the electricity utility are given in Fig. 5 from the PJM database [34], while the gas price is fixed at 0.0571 \$/kW in all time slots [17].

4.2. Distributed algorithm performance

First, we validate the convergence performance of the ADMM-based distributed algorithm for solving the day-ahead scheduling problem. We set $\epsilon = 10^{-3}$ in the stop condition (44). As shown in Fig. 6, the pink line indicates the convergence process of the social operation cost of the MMG network obtained by the ADMM-based distributed algorithm, and the green line represents the optimal solution obtained by Gurobi in a centralized manner. Fig. 6 demonstrates that the proposed distributed algorithm is able to converge to the centralized optimum value 245.4777 \$ after around the 30th iteration, which shows a high speed of convergence. Meanwhile, Fig. 7 presents the convergence process of the primal residual. A smaller primal residual indicates that the solution returned by the distributed algorithm is more accurate. The results show that the proposed distributed algorithm can provide an accurate solution to the day-ahead scheduling problem.

These demonstrate the effectiveness of the proposed distributed algorithm in solving the day-ahead scheduling problem. The optimal operation costs of microgrids 1, 2, and 3 are 81.2556 \$, 77.1676 \$, and 87.0545 \$, respectively. Hereafter, the simulation results of the proposed energy management strategy are given by the results after the day-ahead and intra-day phases.

4.3. Comparison of different scenarios

Four cases are considered to analyze the performance of the proposed energy management strategy:

Case 1: Without consideration of demand response of microgrids and electricity sharing among microgrids;
Case 2: Without consideration of electricity sharing among microgrids, considering demand response of microgrids;
Case 3: Without consideration of demand response of microgrids, considering electricity sharing among microgrids;

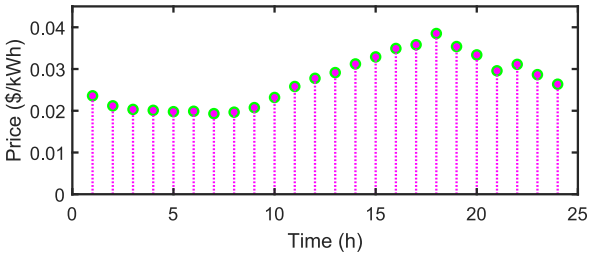

Fig. 5. Electricity prices of the electricity utility.

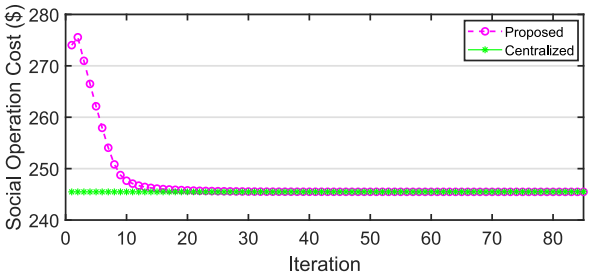

Fig. 6. Social operation cost for the MMG network.

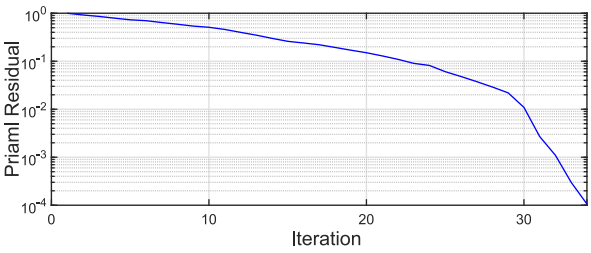

Fig. 7. Primal residuals of the distributed algorithm.

Table 3
Scenario settings (Y: YES; N: NO).

Scenarios	Demand response	Electricity sharing
Case 1 [17]	N	N
Case 2 [21]	Y	N
Case 3 [9]	N	Y
Proposed	Y	Y

4.3.1. Proposed

Considering both demand response of microgrids and electricity sharing among microgrids.

Table 3 shows the comparison of these four different scenarios. Table 4 summarizes their comparison in terms of operation costs, carbon emissions, and wind curtailment. It can be seen that the proposed strategy achieves zero wind curtailment and significantly reduces carbon emissions for all microgrids. In our strategy, microgrids 1, 2, and 3 have 43.64%, 39.98%, and 20.62% carbon emissions reduction compared with Case 1. Moreover, our strategy has the lowest operation cost compared with the other cases. For example, compared with Cases 1, 2, and 3, the proposed strategy reduces the operation costs of microgrid 1 by 17.65%, 14.07%, and 1.53%, respectively. The comparison results demonstrate that integrated demand response and electricity sharing play vital roles in reducing operation costs, carbon emissions, and wind curtailment.

4.4. Optimal electricity sharing

Fig. 8 demonstrates the optimal electricity sharing results under the proposed strategy. The positive values mean that the electricity goes from the former microgrid to the latter one, while the negative values mean the opposite direction. As observed, microgrids actively exchange electricity with each other. Due to the variety of wind power generation and load profiles for different microgrids, each microgrid will be an electricity supplier or receiver in different time slots. For example, microgrid 1 sends electricity out most of the time during the night, while microgrid 2 does so in hours 8–17 and microgrid 3 in hours 12–23. As discussed above, under the electricity sharing setting, the proposed energy management strategy is beneficial for each microgrid in both economic and environmental aspects.

4.5. The impact of CRRs

Fig. 9 demonstrates the impact of CRRs in two cases: with and without electricity sharing among the microgrids. We consider four different CRRs (0%, 10%, 20%, and 30%) and analyze their impact on the operation costs and carbon emissions of the three microgrids. It is obvious that the amount of carbon emissions decreases when the CRR increases. Moreover, the resulting reduction of carbon emissions is proportional to the parameter of CRRs, which demonstrates that the carbon emission limitations (23) are always binding in the cost-minimizing problems. With the increase of the CRR, the operation costs increase in both the two cases. It is because the operation flexibility of microgrids is reduced with the increase of the CRR. Correspondingly, the operation costs of three microgrids are increased.

4.6. Storage dynamics

Fig. 10 and Fig. 11 illustrate the charging and discharging power and SOCs of electric and heat storages in the microgrids. In Fig. 10, the electric storages of the three microgrids work in a charging mode when electricity prices are relatively lower (e.g., at midnight and early morning). Instead, the electric storages work in a discharging mode, when electricity prices are relatively higher (e.g., in the late afternoon and early evening). This can help lower the operation costs of the microgrids. As shown in Fig. 11, the heat storages are generally charged when there is redundant wind power generation and discharged when heat is highly demanded. In this way, the microgrids can make full use of the RESs.

Table 4
Comparison of different scenarios.

MG	Scenarios	Operation costs ($)	Carbon emissions (kg)	Wind Curtailment (kW)
MG 1	Case 1	98.650 4	817.681 6	313.842 1
	Case 2	94.539 8	771.204 9	220.152 0
	Case 3	82.504 8	486.520 9	0
	Proposed	81.239 1	460.842 6	0
MG 2	Case 1	93.180 0	833.086 1	312.520 5
	Case 2	89.067 7	792.357 5	223.246 2
	Case 3	79.094 3	539.553 4	0
	Proposed	76.479 2	500.025 0	0
MG 3	Case 1	103.037 5	923.223 4	315.623 0
	Case 2	99.067 3	893.285 1	232.866 9
	Case 3	88.591 9	796.067 1	0
	Proposed	82.560 6	732.829 5	0

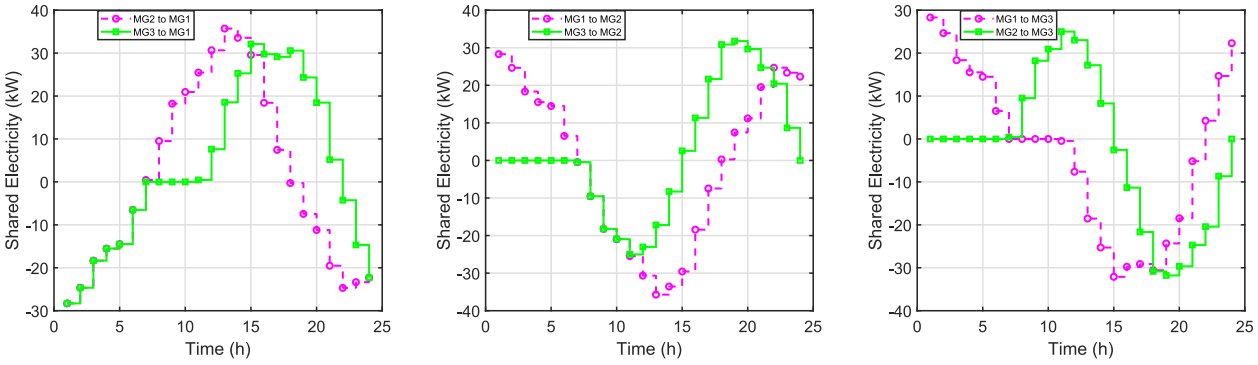

Fig. 8. The amounts of electricity shared among the microgrids.

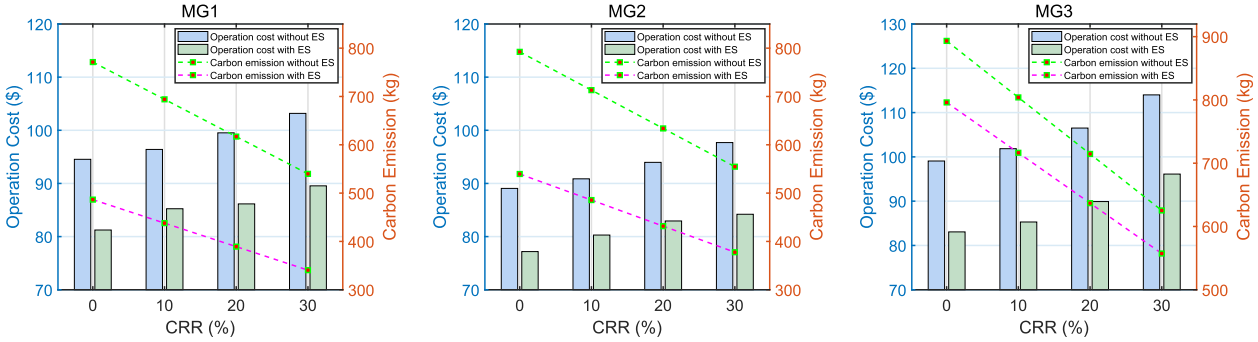

Fig. 9. Impacts of CRR for the three microgrids (ES: electricity sharing).

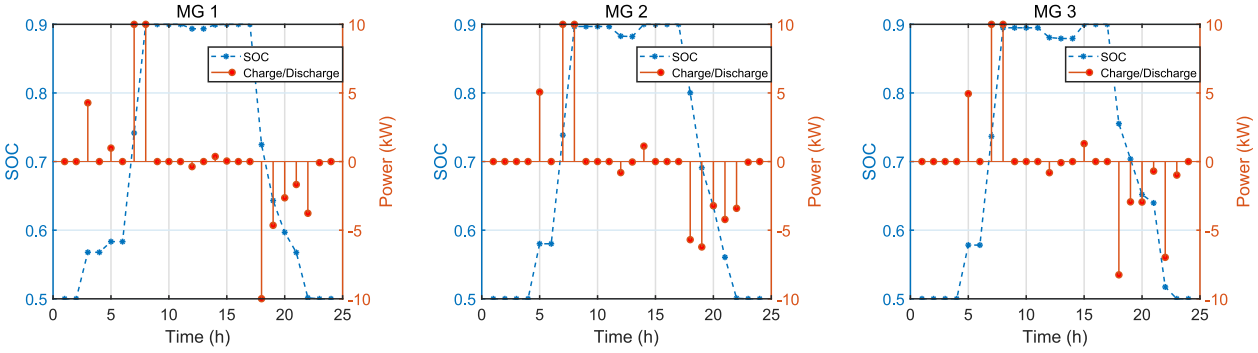

Fig. 10. Electric storage power and SOC in the three microgrids.

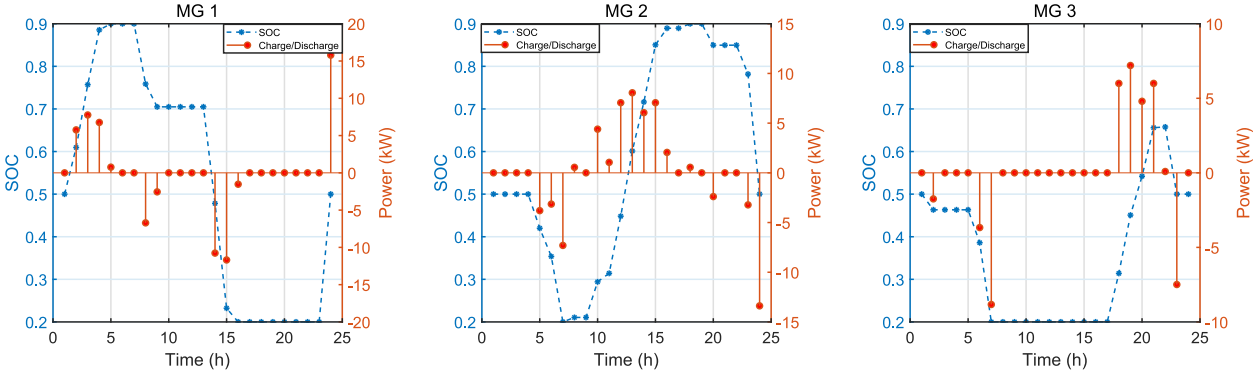

Fig. 11. Heat storage power and SOC dynamics in the three microgrids.

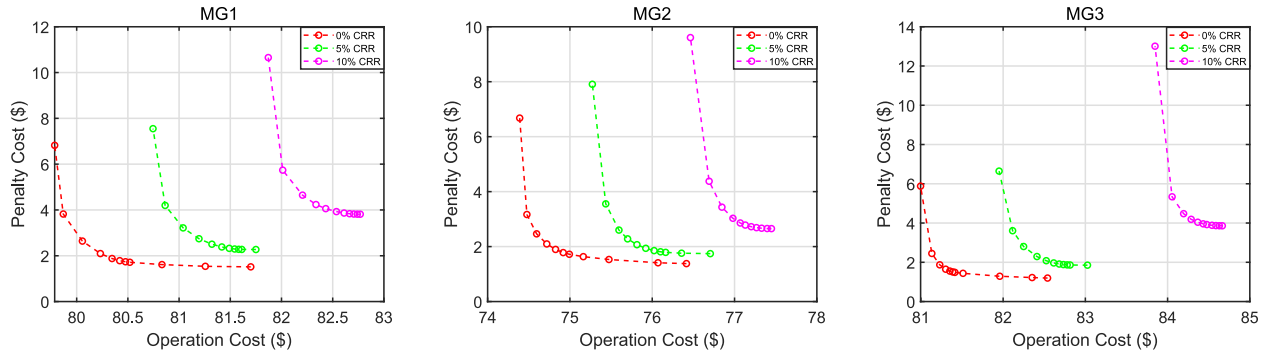

Fig. 12. The trade-off between the operation costs and penalty costs under different CRRs.

4.7. Trade-off between the operation costs and penalty costs

Fig. 12 illustrates the trade-off between the operation costs and penalty costs in the intra-day rescheduling phase with different CRRs $\lambda_i^{CRR} = \{0\%, 5\%, 10\%\}$. The Pareto optimal trade-off curves between operation costs and penalty costs are formed by varying θ from 0 to 1. It can be observed that the penalty costs increases and the operation costs diminishes as $\theta \to 1$, and we have the opposite as $\theta \to 0$. When $\theta = 1$, the operation costs reach their minimum values. When $\theta = 0$, the penalty costs get their minimal results. Fig. 11 also shows the effects of the CRR on this trade-off. We can see that the Pareto optimal trade-off curve moves toward large values as the CRR increases. It is because the flexibility of the microgrids is reduced with an increasing CRR, pulling up the operation costs and penalty costs of each microgrid.

5. Conclusions

This paper proposes an optimal energy management strategy for an MMG network considering carbon emission limitations. The strategy is composed of two parts, the day-ahead scheduling phase and the intra-day rescheduling phase. In the day-ahead phase, we design a distributed algorithm based on ADMM to minimize the social operation cost of the MMG network. The algorithm can settle the electricity sharing between different microgrids without disclosing private information of the microgrids. The uncertainties of RES generation and load demands are addressed in the intra-day phase with the objective of minimizing a weighted sum of operation costs and penalty costs for each microgrid. According to the simulation results, the proposed strategy can achieve optimal energy scheduling for MMG networks with great performances in both economic and environmental aspects. Compared with previous researches, this paper promotes the research on MMG networks in (1) proposing a new energy management strategy for MMG networks considering carbon emission limitations; (2) dealing with the uncertainties of RES generation and load demands through the separation of day-ahead and intra-day phases; and (3) preserving the privacy of microgrids using a distributed algorithm. According to the simulation cases based on the MMG network, we find that the settings of CRR have significant impact on the operation costs and carbon emissions of microgrids. Thus, a method to determine reasonable CRRs for microgrids is important, but it is not studied in this paper. In the future research, we will consider to develop a CRR determination method and examine its impact on MMG scheduling.

Credit author statement

Xiaoqing Zhong: Conceptualization, Methodology, Software, Writing - Original draft preparation. **Weifeng Zhong:** Methodology, Writing - Reviewing and Editing. **Yi Liu:** Writing - Reviewing and Editing. **Chao Yang:** Writing - Reviewing and Editing. **Shengli Xie:** Supervision.

Declaration of competing interest

The authors declare that they have no known competing financial interests or personal relationships that could have appeared to influence the work reported in this paper.

Acknowledgements

This work was supported in part by the National Natural Science Foundation of China under Grant 62003099, Grant 61973087, and Grant U1911401; in part by the Guangdong Basic and Applied Basic Research Foundation under Grant 2019A1515011377, and Grant 2019A1515011114; and in part by the State Key Laboratory of Synthetical Automation for Process Industries under Grant 2020-KF-21-02.

References

[1] Sinha RK, Chaturvedi ND. A review on carbon emission reduction in industries and planning emission limits. Renew Sustain Energy Rev 2019;114:109304.
[2] Zhang X, Wang Y. How to reduce household carbon emissions: a review of experience and policy design considerations. Energy Pol 2017;102:116–24.
[3] Isuru M, Krishnan A, Foo EY, Gooi HB. Framework for network-constrained cooperative trading of multi-microgrid systems. In: 2020 59th IEEE conference on decision and control (CDC). IEEE; 2020. p. 1347–54.
[4] Wang H, Huang J. Incentivizing energy trading for interconnected microgrids. IEEE Trans Smart Grid 2016;9(4):2647–57.
[5] Cui S, Wang Y-W, Xiao J-W. Peer-to-peer energy sharing among smart energy buildings by distributed transaction. IEEE Trans Smart Grid 2019;10(6):6491–501.
[6] Tushar W, Saha TK, Yuen C, Smith D, Poor HV. Peer-to-peer trading in electricity networks: an overview. IEEE Trans Smart Grid 2020;11(4):3185–200.
[7] Mengelkamp E, Gärttner J, Rock K, Kessler S, Orsini L, Weinhardt C. Designing microgrid energy markets: a case study: the brooklyn microgrid. Appl Energy 2018;210:870–80.
[8] Zhong W, Xie S, Xie K, Yang Q, Xie L. Cooperative p2p energy trading in active distribution networks: an milp-based nash bargaining solution. IEEE Trans Smart Grid 2020;12(2):1264–76.
[9] Chen Y, Wei W, Liu F, Wu Q, Mei S. Analyzing and validating the economic efficiency of managing a cluster of energy hubs in multi-carrier energy systems. Appl Energy 2018;230:403–16.
[10] Mirzapour-Kamanaj A, Majidi M, Zare K, Kazemzadeh R. Optimal strategic coordination of distribution networks and interconnected energy hubs: a linear multi-follower bi-level optimization model. Int J Electr Power Energy Syst 2020;119:105925.
[11] Yang Z, Hu J, Ai X, Wu J, Yang G. Transactive energy supported economic

operation for multi-energy complementary microgrids. IEEE Trans Smart Grid 2020;12(1):4–17.
[12] Hoehne CG, Chester MV. Optimizing plug-in electric vehicle and vehicle-to-grid charge scheduling to minimize carbon emissions. Energy 2016;115:646–57.
[13] Tu R, Gai YJ, Farooq B, Posen D, Hatzopoulou M. Electric vehicle charging optimization to minimize marginal greenhouse gas emissions from power generation. Appl Energy 2020;277:115517.
[14] Ugurlu A. An emission analysis study of hydrogen powered vehicles. Int J Hydrogen Energy 2020;45(50):26522–35.
[15] Ren L, Zhou S, Ou X. Life-cycle energy consumption and greenhouse-gas emissions of hydrogen supply chains for fuel-cell vehicles in China. Energy 2020;209:118482.
[16] Kamboj A, Chanana S. Optimization of cost and emission in a renewable energy micro-grid. In: 2016 IEEE 1st international conference on power electronics, intelligent control and energy systems (ICPEICES). IEEE; 2016. p. 1–6.
[17] Yi JH, Ko W, Park J-K, Park H. Impact of carbon emission constraint on design of small scale multi-energy system. Energy 2018;161:792–808.
[18] Hua W, Jiang J, Sun H, Wu J. A blockchain based peer-to-peer trading framework integrating energy and carbon markets. Appl Energy 2020;279:115539.
[19] Feng P, He X. Mixed neurodynamic optimization for the operation of multiple energy systems considering economic and environmental aspects. Energy 2021:120965.
[20] Cheng Y, Zhang N, Wang Y, Yang J, Kang C, Xia Q. Modeling carbon emission flow in multiple energy systems. IEEE Trans Smart Grid 2018;10(4):3562–74.
[21] He L, Lu Z, Geng L, Zhang J, Li X, Guo X. Environmental economic dispatch of integrated regional energy system considering integrated demand response. Int J Electr Power Energy Syst 2020;116:105525.
[22] Hu J, Zhou H, Li Y, Hou P, Yang G. Multi-time scale energy management strategy of aggregator characterized by photovoltaic generation and electric vehicles. J Mod Power Syst Clean Energy 2020;8(4):727–36.
[23] Su J, Lie T, Zamora R. A rolling horizon scheduling of aggregated electric vehicles charging under the electricity exchange market. Appl Energy 2020;275:115406.
[24] Hou W, Liu Z, Ma L, Wang L. A real-time rolling horizon chance constrained optimization model for energy hub scheduling. Sustain Cities Soc 2020;62:102417.
[25] Palma-Behnke R, Benavides C, Lanas F, Severino B, Reyes L, Llanos J, Sáez D. A microgrid energy management system based on the rolling horizon strategy. IEEE Trans Smart Grid 2013;4(2):996–1006.
[26] W. Zhong, K. Xie, Y. Liu, S. Xie, L. Xie, Chance constrained scheduling and pricing for multi-service battery energy storage, IEEE Trans Smart Grid.
[27] Tan O, Gündüz D, Vilardebó JG. Optimal privacy-cost trade-off in demand-side management with storage. In: 2015 IEEE 16th international workshop on signal processing advances in wireless communications (SPAWC). IEEE; 2015. p. 370–4.
[28] Boyd S, Parikh N, Chu E. Distributed optimization and statistical learning via the alternating direction method of multipliers. Now Publishers Inc; 2011.
[29] Fletcher R, Leyffer S. Numerical experience with lower bounds for miqp branch-and-bound. SIAM J Optim 1998;8(2):604–16.
[30] Bemporad A. Solving mixed-integer quadratic programs via nonnegative least squares. IFAC-PapersOnLine 2015;48(23):73–9.
[31] Gurobi Optimization, LLC. Gurobi optimizer reference manual. 2021 [Online]. Available: https://www.gurobi.com.
[32] Zhao Z, Guo J, Lai CS, Xiao H, Zhou K, Lai LL. Distributed model predictive control strategy for islands multimicrogrids based on noncooperative game. IEEE Trans Ind Inf 2020;17(6):3803–14.
[33] Ju L, Tan Q, Lin H, Mei S, Li N, Lu Y, Wang Y. A two-stage optimal coordinated scheduling strategy for micro energy grid integrating intermittent renewable energy sources considering multi-energy flexible conversion. Energy 2020;196:117078.
[34] Pjm real-time hourly lmps [Online]. Available: https://dataminer2.pjm.com/feed/rt_hrl_lmps/definition.